# Gold clusters on thiol-functionalized Fe₃O₄@SiO₂ nanoparticles: a novel bioreduced catalyst for oxidation of benzyl alcohol

Suhaila Borhamdin[a], Mustaffa Shamsuddin[a,b], Abdolhamid Alizadeh[b,c]

[a] *Department of Chemistry, Faculty of Science, Universiti Teknologi Malaysia, 81310 UTM Johor Bahru, Johor, Malaysia.*
[b] *Ibnu Sina Institute for Fundamental Science Studies, Universiti Teknologi Malaysia, 81310 UTM Johor Bahru, Johor, Malaysia.*
[c] *Department of Chemistry & Nanoscience and Nanotechnology Research Center (NNRC), Razi University, Kermanshah 67149, Iran..*

*\*Corresponding Author: mustaffas@utm.my; ahalizadeh2@hotmail.com*

**GRAPHICAL ABSTRACT**

**ABSTRACT**

Bioinspired synthesis of a magnetically recoverable gold nanoparticles (AuNPs) catalysts on Fe₃O₄@SiO₂ support is reported. Firstly, AuNPs was prepared by using the aqueous leaf extract of *Polygonum minus* (kesum) as a reducing and stabilizing agent. The reduction of $Au^{3+}$ ions to elemental Au was rapidly occurred and completed within 20 minutes at room temperature. The bioreduction process was monitored by UV-vis spectroscopy and the AuNPs were characterized by FTIR, XRD, TEM, and CV analyses. Then, same bioreduction process was employed in the preparation of Au catalysts supported on thiol-functionalized silica-coated magnetite nanoparticles. The supported Au catalysts were characterized by FTIR, XRD, TEM, XPS and AAS analyses. The performance of bioreduced supported Au catalysts was evaluated in the liquid phase oxidation of benzyl alcohol to benzaldehyde in water at 80° C using $H_2O_2$ as oxidant, reaction time of 6 h and 8 mg (4 µmol Au) of catalyst. Under these conditions, benzyl alcohol conversion of 58% and benzaldehyde selectivity of 100% with TON of 4,205 were achieved. The supported Au catalyst is stable and can be recovered and reused for three times without a significant loss in its activity and selectivity.

*Keywords*: *Polygonum minus*, Au catalyst, oxidation, benzyl alcohol

## 1. INTRODUCTION

Noble metals such as Pt, Pd, Au, Ag, Ru, and Rh are widely used as heterogeneous catalyst. However, much effort has been focused on AuNPs catalysts due to their excellent catalytic performance in terms of high activity and selectivity especially for liquid phase oxidation of alcohols [1].

Traditionally, AuNPs preparation is carried out via chemical procedures that employ toxic and poisonous chemicals [2, 3]. Recently, the utilization of biological systems has appeared as a novel and reliable method for the synthesis of AuNPs due to a growing demand to develop eco-friendly processes in nanomaterials syntheses. A biosynthetic method for AuNPs preparation employing plant extract has emerged as a green, simple and viable alternative to traditional chemical procedures that employ toxic and poisonous chemicals [4].

*Polygonum minus* (kesum) is locally available herbs in Malaysia that have been reported to contain high phenolic compounds and antioxidant activity, thus have great potential to be used as a reducing agent in the preparation of metal nanoparticles such as AuNPs [5].

Generally, supported AuNPs catalysts are prepared by the deposition–precipitation or co-precipitation methods and the particle sizes are adjusted by varying experimental parameters, such as the pH, reducing agent, concentration of precursors in solution and temperature. However, the surfaces of acid or hydrophobic supports, such as SiO₂ and activated carbon are not suitable for the deposition of anionic species [6]. Therefore, the ligand assisted methods using the organofunctional alkoxysilanes containing functionalities such as thiol (-SH) groups to covalently anchor AuNPs onto the solid support have more advantages [7].

In addition to the problem of synthesizing and stabilizing of AuNPs, an issue that need attention is the difficulty arising from size reduction and the challenges of separating very small particles of AuNPs catalyst, most of the time in a colloidal equilibrium, from the products. In this regard, AuNPs have been dispersed on solid supports to facilitate the catalyst recovery and increase the catalyst

stability [8, 9]. As the size of the support decreases, separation using physical methods, such as filtration or centrifugation, becomes a difficult and time-consuming procedure. Simple filtration is inefficient to accomplish product isolation in systems comprised of nanoparticles stabilized in solution or in very thin solids. Thus the use of magnetically recoverable solid supports such as magnetite ($Fe_3O_4$) nanoparticles is proposed [6, 10, 11].

Herein, the biosynthesis of magnetically recoverable AuNPs catalysts on $Fe_3O_4@SiO_2$ support is reported. The AuNPs was prepared by using the aqueous leaf extract of *Polygonum minus* (kesum) as a reducing and stabilizing agent. Then, same bioreduction process was employed in the preparation of Au catalysts supported on thiol-functionalized silica-coated magnetite nanoparticles. The performance of bioreduced supported Au catalysts was evaluated in the liquid phase oxidation of benzyl alcohol to benzaldehyde.

## 2. EXPERIMENTS

### 2.1 Materials

All chemicals were purchased commercially from Merck, Sigma-Aldrich or Fluka and were used as received without any purification. Fresh leaves of *Polygonum minus* were purchased from a local market in Johor. Commercial grade solvents used in the synthesis were dried using appropriate drying agents.

### 2.2 Preparation of Polygonum Minus Leaf Extract

*Polygonum minus* leaves were washed several times with deionized water to remove dust and allowed to dry at room temperature for 1 week. 2 g of finely powdered leaves were mixed with 100 mL of deionized water in a beaker. Then, the mixture was boiled for 10 minutes, filtered and stored at 5 $^{\circ}$C for further experiments. The powdered leaves were then characterized by FTIR spectroscopy.

### 2.3 Preparation of Magnetite (Fe₃O₄) Nanoparticles

Magnetite ($Fe_3O_4$) nanoparticles were prepared via co-precipitation of $Fe^{3+}$ and $Fe^{2+}$ ions [12]. $FeSO_4.7H_2O$ (1.3901 g; 5 mmol) was dissolved in 50 mL of deionized water and mixed with 50 mL solution of $FeCl_3.6H_2O$ (2.8 g; 10 mmol) in deionized water. The mixture was stirred followed by addition of NaOH (14.5 mL; 3 M) at 30 $^{\circ}$C until the mixture reached a pH around 11. Then the mixture was heated to 80 $^{\circ}$C for 30 minutes. The $Fe_3O_4$ nanoparticles were isolated from the solution by magnetic separation using neodymium magnet bar and washed with deionized water until pH 7 reached. Finally, the $Fe_3O_4$ nanoparticles were dried in vacuum dessicator. The solid

products obtained were then characterized by FTIR, FESEM, and XRD analyses.

### 2.4 Preparation of Silica-Coated Magnetite (Fe₃O₄-SiO₂)

Silica-coated magnetite was prepared via microemulsion technique [13]. 20 mL of polyoxyethylene(5) isooctylphenyl ether (IGEPAL) was dispersed in 300 mL of cyclohexane. Then, 100 mg of $Fe_3O_4$ dispersed in 40 mL of cyclohexane was added. The mixture was stirred at room temperature until it became transparent. Then, 5 mL of ammonium hydroxide (29% aqueous solution) was added followed by 4 mL of tetraethylorthosilicate (TEOS) and the solution was stirred for 16 hours. The $Fe_3O_4$-$SiO_2$ nanoparticles were precipitated with methanol followed by centrifugation at 4000 rpm for 30 minutes. Finally, after being washed with ethanol, the $Fe_3O_4$-$SiO_2$ nanoparticles were dried in vacuum dessicator. The solid products obtained were then characterized by FTIR, FESEM, and XRD analyses.

### 2.5 Preparation of Thiol-Functionalized Silica-Coated Magnetite (Fe₃O₄-SiO₂-SH)

100 mg of $Fe_3O_4$-$SiO_2$ nanoparticles were dispersed in 15 mL of dried toluene. Then, 1 mL of 3-mercaptopropyl-trimethoxysilane (MPTMS) was added. The mixture was stirred for 2 hours at room temperature and under nitrogen atmosphere. The $Fe_3O_4$-$SiO_2$-SH nanoparticles were isolated from the solution by magnetic separation using neodymium magnet bar and washed with dried toluene. Finally, the solid products were dried in vacuum dessicator. The solid products obtained were then characterized by FTIR, XRD, TEM and elemental CHNS analyses. Anal. Found: C, 2.66; H, 1.29; S, 2.08.

### 2.6 Preparation of Supported Gold(III) on Thiol-Functionalized Silica-Coated Magnetite (Fe₃O₄-SiO₂-SH-Au(III))

39 mg of $Fe_3O_4$-$SiO_2$-SH were added to aqueous solution of $HAuCl_4$ (10 mL; 2.5 mM). The mixture was stirred at room temperature for 3 hours. The $Fe_3O_4$-$SiO_2$-SH-Au(III) nanoparticles were then magnetically collected from the solution, washed with deionized water and finally dried in vacuum dessicator. Then, the solid products obtained were characterized by AAS analysis.

### 2.7 Preparation of Supported Gold(0) on Thiol-Functionalized Silica-Coated Magnetite (Fe₃O₄-SiO₂-SH-Au(0))

39.7 mg of $Fe_3O_4$-$SiO_2$-SH-Au(III) were added to the aqueous leaf extract of *Polygonum minus* (4 mL extract diluted into 20 mL with deionized water). The colour of the mixture changed from orange to brown after few minutes,

indicating the formation of AuNPs. The mixture was stirred at room temperature for 1 hour. Then, the brown $Fe_3O_4$-$SiO_2$-SH-Au(0) nanoparticles were magnetically collected from the solution, washed with deionized water and finally dried in vacuum dessicator. Finally, the solid products obtained were characterized by FTIR, XRD, TEM and AAS analyses.

## 2.8 Characterization

FTIR spectra were recorded on a Shimadzu FTIR 8300 spectrometer in the range of 4000 to 400 cm$^{-1}$ at room temperature. XRD analyses were performed on a Bruker D8 Advance diffractometer with Cu-Kα radiation in the range of 2θ between 10$^o$ and 90$^o$. High-resolution TEM images of the samples were recorded with a JEOL JEM-2100 microscope operated at 200kV and equipped with an energy-dispersive X-ray spectrometer (EDS). The high-resolution FESEM images of the samples were recorded with a JSM-6701F microscope equipped with an energy-dispersive X-ray spectrometer (EDS). Percentage of Au loading on the supported catalyst were determined using a Perkin Elmer-AAnalyst 400 atomic absorption spectrometer. Elemental CHNS analyses were performed using a Thermo Finnigan Eager 300 CHNS analyzer. GC analyses for the catalysis product were carried out by using an Agilent Technologies 7890A GC system equipped with a 30 m x 0.320 mm x 0.25 µm HP-5 capillary column and a flame ionization detector (FID).

## 2.9 Oxidation Reaction of Benzyl Alcohol

Benzyl alcohol (3 mL; 29 mmol), hydrogen peroxide (1 mL; 36 mmol), supported catalyst $Fe_3O_4$-$SiO_2$-SH-Au(0) (8 mg; 4 µmol Au) and water (6 mL) were mixed together in a test tube. The mixture was placed in a Radleys 12-placed reaction carousel. The mixture was stirred at 80 $^o$C for 6 hours with temperature carefully controlled by a contact thermometer (± 1 $^o$C). Then, the catalyst was magnetically recovered by placing a neodymium magnet bar on the reactor wall and the products were collected and analyzed by GC-FID. Then, recovered catalyst was washed with 2 mL of ethanol inside the reactor and dried under vacuum. The catalyst was then reused for second time by adding new portion of solvent, oxidant and substrate. Besides, the control experiment with the absence of supported Au catalyst has also been carried out.

## 3. RESULTS AND DISCUSSION

The magnetically recoverable support used in this study consists of core–shell silica-coated magnetite nanoparticles ($Fe_3O_4$-$SiO_2$). The magnetite nanoparticles cores ($Fe_3O_4$) were synthesized by the coprecipitation method [12]. Then, the magnetite nanoparticles were spherically coated with silica by microemulsion technique [13]. The silica spheres were later functionalized with 3-mercaptopropyl-trimethoxysilane (MPTMS) to improve the uptake of $Au^{3+}$ ions from the $HAuCl_4$ aqueous solution. The metal-loaded solid was then subjected to reduction with *Polygonum minus* leaf aqueous extract under optimized conditions, resulted in the anchoring of Au(0) nanoparticles on the surface of the thiol-functionalized silica coated magnetic support.

From the elemental CHNS analysis results, it was found that there are 0.6499 mmol of 3-mercaptopropyl-trimethoxysilane (MPTMS) molecules in every 1 gram sample of $Fe_3O_4$-$SiO_2$-SH. The molar ratio of Au(III) used in further reaction was calculated based on this SH loading. The data obtained from the AAS analysis showed that the amount of Au metal present in the supported Au catalyst ($Fe_3O_4$-$SiO_2$-SH-Au(0)) is 9.0 wt%. From this data, it was calculated that there is 0.4569 mmol Au in every 1 gram sample of supported Au catalyst ($Fe_3O_4$-$SiO_2$-SH-Au(0)). This data also indicates that 70% of the thiol groups have covalently bonded with Au metal. The catalyst loading used in the catalytic studies was calculated based on this Au metal loading. Besides, it was also found that only 1% of Au was immobilized when the support was not functionalized with thiol groups. This result confirmed the very low affinity of the silica surfaces for $Au^{3+}$ ions which is consistent with other previous reports [6, 13].

## 3.1 FESEM Studies

The morphology of the magnetite nanoparticles ($Fe_3O_4$) and the silica-coated magnetite nanoparticles ($Fe_3O_4$-$SiO_2$) were examined by field emission scanning electron microscopy (FESEM). The FESEM image of the synthesized magnetite nanoparticles ($Fe_3O_4$) is shown in Figure 1. It is observed that the magnetite nanoparticles are of irregular shape with an average particles size of about 14.3 nm by manual analysis of 60 particles using ImageJ software.
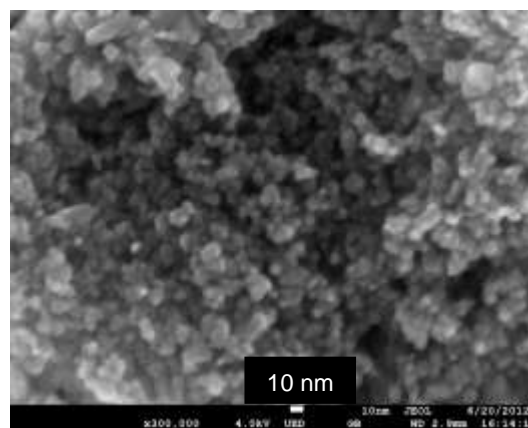


Figure 1. FESEM images of $Fe_3O_4$ nanoparticles

Meanwhile the Figure 2 showed the FESEM image of the synthesized silica-coated magnetite nanoparticles. It is clear that the structure of silica-coated magnetite nanoparticles is spherical with a smooth surface. The average particles size calculated by manual analysis of 50 particles using ImageJ software is about 20.0 nm. Therefore, the average thickness of silica coating layer on the magnetite surface is about 2.9 nm ((silica-coated magnetite size - magnetite size)/ 2).
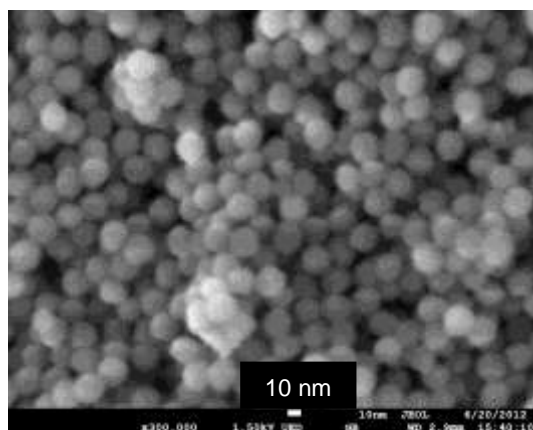


Figure 2. FESEM images of $Fe_3O_4$-$SiO_2$ nanoparticles

### 3.2 TEM Studies

The morphology of the thiol-functionalized silica-coated magnetite ($Fe_3O_4$-$SiO_2$-SH) and the supported Au catalyst ($Fe_3O_4$-$SiO_2$-SH-Au(0)) were further analyzed by transmission electron microscopy (TEM). Figure 3(a) illustrated the TEM images of $Fe_3O_4$-$SiO_2$-SH nanoparticles. The nanoparticles contain a layer of silica coating on the surface of magnetite. Although most of the particles appear as spherical in shape, some agglomeration can be seen and thus the particle size cannot be precisely determined. In addition, the particles are not uniformly in core-shell structure, which may due to agglomeration of the magnetite nanoparticles during the coating process.

The TEM image of $Fe_3O_4$-$SiO_2$-SH-Au(0) in Figure 3(b) showed that the AuNPs were immobilized on the thiol-functionalized silica-coated magnetite support. Some agglomeration can still be seen and the overall particles size cannot be precisely determined. However, the average Au particles size calculated by manual analysis of 20 Au particles using ImageJ software is about 1.4 nm. From previous studies, there are few papers have reported the formation of supported AuNPs with particles size less than 5 nm. Wu *et al.* [14] have successfully immobilized AuNPs on the thiol-functionalized porous silica with AuNPs size in the range of 2-4 nm. Meanwhile, Zhu *et al.* [15] have reported the AuNPs supported on amine-functionalized SBA-15 with particles size around 3 nm. Although the same reduction condition has been used for supported

AuNPs, it produce smaller particles size as compared to the unsupported AuNPs. This can be explained by the effect of thiol ligand employed which has covalently anchored AuNPs onto the solid support and therefore keep them stable by steric or electrostatic stabilization, control the size of AuNPs, avoid the agglomeration and increase the AuNPs dispersion on the solid support [7].
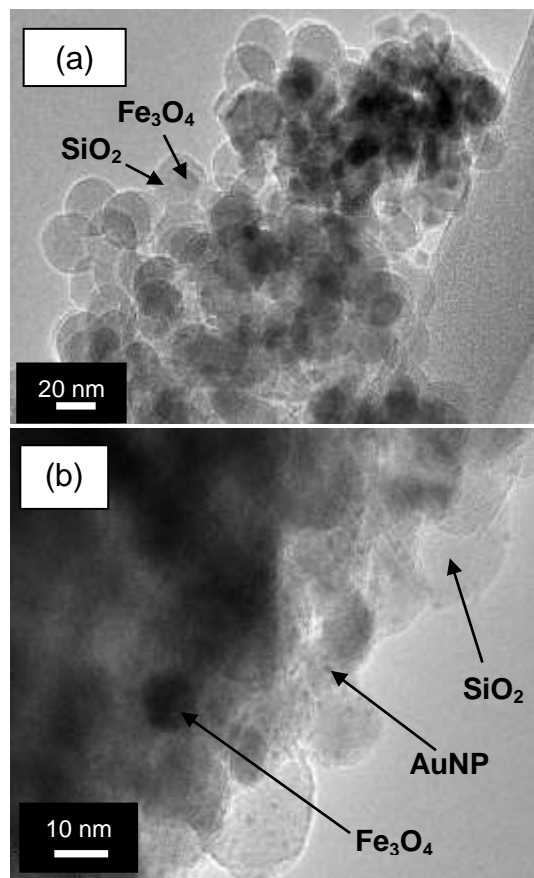


Figure 3. (a) TEM images of $Fe_3O_4$-$SiO_2$-SH and (b) TEM image of $Fe_3O_4$-$SiO_2$-SH-Au(0).

### 3.3 X-ray Diffraction Analysis

X-ray diffraction (XRD) technique has been used to confirm the crystalline structure of magnetite and the supported AuNPs. The XRD pattern of crystalline magnetite nanoparticles is shown in Figure 4(a). The diffraction peaks of (2 2 0), (3 1 1), (4 0 0), (4 2 2), (5 1 1) and (4 4 0) reflect the magnetite crystal with a cubic spinel structure [12]. The unit cell of cubic spinel structure consists of eight ferric ions at tetrahedral sites (A sites) each with four oxide ions nearest neighbours, and eight ferric ions and eight ferrous ions at octahedral sites (B sites) each with six oxide ions as the nearest neighbours. This system could be referred to the structural formula of $(Fe^{3+})_A[Fe^{2+}Fe^{3+}]_B O_4$ [16]. The peak corresponding to the (311) plane is more intense than the other planes suggesting that (311) is the predominant orientation. Figure 4(b)

showed the XRD pattern of silica-coated magnetite nanoparticles. It is clearly observed that the XRD result of silica-coated magnetite nanoparticles and pure magnetite are mostly coincident except a broader peak at 2θ of about 23.5° originating from amorphous silica [17].

Furthermore, by comparing the XRD pattern of supported AuNPs on thiol-functionalized silica-coated magnetite in Figure 4(c) with the corresponding unsupported AuNPs (Figure 4(d)), the XRD pattern of supported AuNPs display the same three peaks that can be identified as the (1 1 1), (2 0 0), and (2 2 0) reflection lines of the Au fcc-cubic phase. This indicates that the supported AuNPs are crystalline in structure. Besides that, the XRD pattern of supported AuNPs also shows the characteristic peaks of magnetite support.
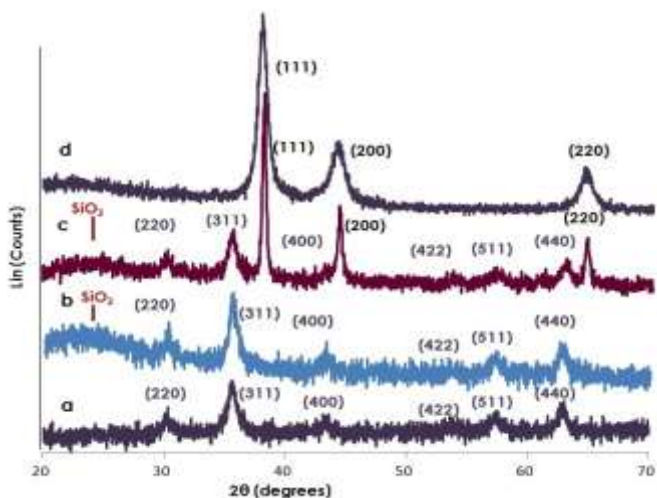


Figure 4. XRD pattern of (a) $Fe_3O_4$ (b) $Fe_3O_4$-$SiO_2$ (c) $Fe_3O_4$-$SiO_2$-SH-Au(0) (d) AuNPs.

*3.4 FTIR Analysis*

The FTIR spectra of $Fe_3O_4$, $Fe_3O_4$-$SiO_2$, $Fe_3O_4$-$SiO_2$-SH, *Polygonum minus* leaf powder and $Fe_3O_4$-$SiO_2$-SH-Au(0) are displayed in Figure 5. As show in FTIR spectrum (a), the characteristic absorption band of Fe-O bonds in magnetite ($Fe_3O_4$) appears at 582 cm$^{-1}$ [12]. The broad absorption band at 3391 cm$^{-1}$ was due to O-H stretching vibration, which corresponds to hydroxyl groups on the surface of iron oxide and this band can be assigned to the adsorbed water molecules [18]. While in FTIR spectrum (b), the characteristic absorption bands of silica occur. The band at 1102 cm$^{-1}$ is characteristic peak of the vibration of Si-O-Si and that at 470 cm$^{-1}$ is an indication of the presence of Si-O-Fe [19]. There is also a weak band at 960 cm$^{-1}$ corresponding to the Si-OH bending vibration and a broad absorption band at 3428 cm$^{-1}$ due to O-H stretching vibration from the silanol groups on the surface of silica. The FTIR spectrum (c) showed the functionalization of –$(CH_2)_3$SH is evident from the high wave number part of the

spectrum, where the absorption bands at 2918 cm$^{-1}$ is assigned to the vibrations of $CH_2$ groups. The significant peak which are characteristic of the ν(SH) stretching modes could not be observed due to the little quantity of MPTMS grafted onto silica surface. Besides that, the absorption bands due to Si-OH vibrations of silanol groups has reduced in intensity suggesting that the silica-coated magnetite has been successfully functionalized with 3-mercaptopropyl-trimethoxysilane (MPTMS) [18].

The FTIR spectrum of *Polygonum minus* leaf powder (d) showed characteristic bands for O-H stretching vibrations at 3425 cm$^{-1}$ (polyols), asymmetric stretching vibrations of C-H at 2925 cm$^{-1}$ (aldehydes), stretching vibrations of C=O at 1638 cm$^{-1}$ (amides and aldehydes), stretching vibrations of C-N at 1399 cm$^{-1}$ and stretching vibrations of C-O at 1071 cm$^{-1}$ (polyols) functional groups. It was found that the FTIR spectrum of $Fe_3O_4$-$SiO_2$-SH-Au(0) (e) showed similar peaks as observed in the FTIR spectra (a) to (d). It indicates that the AuNPs have been successfully immobilized on the thiol-functionalized silica-coated magnetite support and some of the biomolecules from the *Polygonum minus* leaf extract may act as a capping agent and stabilized the nanoparticles.

Figure 5. FTIR spectra of (a) $Fe_3O_4$ nanoparticles, (b)
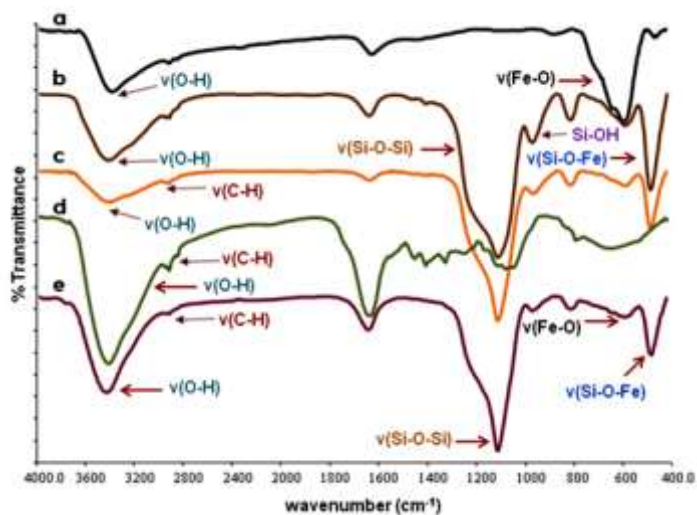


$Fe_3O_4$-$SiO_2$, (c) $Fe_3O_4$-$SiO_2$-SH, (d) *Polygonum minus* leaf powder and (e) $Fe_3O_4$-$SiO_2$-SH-Au(0).

*3.5 Oxidation Reaction of Benzyl Alcohol Using Supported Au Catalyst $Fe_3O_4$-$SiO_2$-SH-Au(0)*

Currently, liquid phase oxidation of benzyl alcohol (BzOH) is the practically preferred reaction route for the production of chlorine-free benzaldehyde (BzH) with high selectivity [20]. Therefore, the catalytic oxidation of benzyl alcohol was used to probe the activity and recovery of the supported Au catalyst ($Fe_3O_4$-$SiO_2$-SH-Au(0)). The first

attempt to catalyze the oxidation of benzyl alcohol using the supported Au catalyst synthesized in this study was performed in water at 80 $^o$C using $H_2O_2$ as oxidant, reaction time of 6 h and 8 mg (4 μmol Au) of catalyst without any base or organic solvent. Water has been used as solvent since it could enhance the oxidation process significantly as demonstrated by Yang *et al*. [21]. Under the above reaction conditions, benzyl alcohol conversion of 58% and benzaldehyde selectivity of 100% with 4,205 mol/mol$_{cat}$ turnover number (TON) were achieved. The control experiment in the absence of the supported catalyst gave a slight benzyl alcohol conversion of 10%.

The recyclability of the catalyst in the oxidation of benzyl alcohol under the same conditions was also investigated. After the first run, the catalyst was magnetically recovered by placing a neodymium magnet bar on the reaction tube wall as shown in Figure 6 and the products were collected and analyzed by GC-FID. The recovered catalyst was then washed with ethanol (2 mL) inside the reactor, and dried under vacuum. The catalyst was reused by adding new portion of solvent, oxidant and substrate.
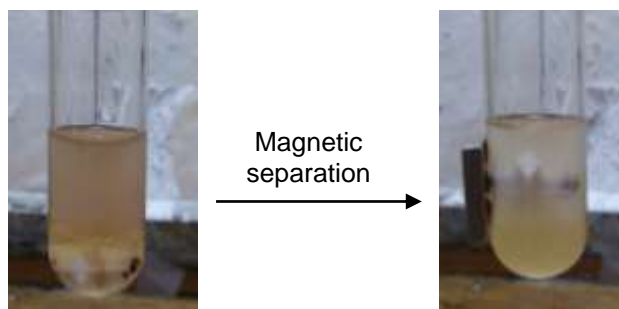


Figure 6. Illustration of magnetic separation of the supported Au catalyst between each reaction batch.

After the 3rd run, the conversion of benzyl alcohol slightly decrease to 50% but the selectivity to benzaldehyde was maintained at 100% as shown in Figure 7.
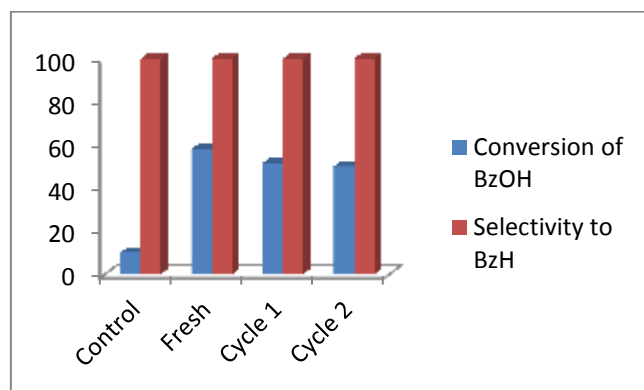


Figure 7. The catalytic performance of recycling bioreduction catalysts. (Conditions: BzOH 29 mmol, $H_2O_2$

36 mmol, catalyst 8 mg, temperature 80 $^\circ$C, time 6 h, Au loading 9.0 wt%).

Zhan *et al*. [20] had first reported the liquid phase oxidation of benzyl alcohol using supported bioreduced Au catalyst on TS-1. They carried out the catalytic experiment in water at 80 $^o$C using $H_2O_2$ as oxidant, reaction time of 6 h with 4.6 μmol Au catalyst. Under these optimal conditions, benzyl alcohol conversion of 67% and benzaldehyde selectivity of 84% with TON of 4,224 were achieved. Therefore, the catalytic performance of the functionalized silica-coated magnetite supported biosynthesized AuNPs catalyst prepared in this study showed comparable conversion but with slightly better selectivity. Significantly, the catalyst recovery using magnetic separation in this study was easier as compared to the common heterogeneous support system.

## 4. CONCLUSION

The biosynthesis method using *Polygonum minus* leaf extract is cost-effective and environmental friendly and can be used in the synthesis of AuNPs instead of using chemical methods. The magnetite supported biosynthesized Au catalyst is able to oxidize benzyl alcohol to benzaldehyde with high activity, high selectivity and above all, environmentally friendly and therefore may have good potential in industrial application. Furthermore, the catalyst recovery using magnetic separation was easier and efficient as compared to conventional filtration method.

## REFERENCES

[1] Hashmi, A. S. K.; Hutchings, G. J. Angew. Chem. Int. Ed. 45 (2006) 7896.
[2] Tan, Y., Dai, Y., Li, Y., Zhua, D. J. Mater. Chem. 13 (2003) 1069.
[3] Iwamoto, M., Kuroda, M., Kanzow, J., Hayashi, S., Faupel, F. Adv. Powder Technol. 16 (2005), 137.
[4] Iravani, S. Green Chem. 13 (2011), 2638.
[5] Huda-Faujan, N., Noriham, A., Norrakiah A. S., Babji, A. S. ASEAN Food Journal 14 (2007) 61.
[6] Oliveira, R. L., Zanchet, D., Kiyohara, P. K., Rossi, L. M. Chem. Eur. J. 17 (2011) 4626.
[7] Costa, N. J. S., Rossi, L. M. Nanoscale 4 (2012) 5826.
[8] Haruta, M. Catal Today. 36 (1997) 153.

[9]   Bond, G. C., Thompson, D. T. Catal. Rev. Sci. Eng. 41 (1999) 319.

[10] Stevens, P. D., Fan, J., Gardimalla, H. M. R., Yen, M., Gao, Y. Org. Lett. 7 (2005) 2085.

[11] Oliveira, R. L., Kiyohara, P. K., Rossi, L. M. (2010). Green Chem. 12 (2010), 144.

[12] Yuan, D., Zhang, Q., Dou, J. Catal. Commun. 11 (2010) 606.

[13] Jacinto, M. J., Kiyohara, P. K., Masunaga, S. H., Jardim, R. F., Rossi, L. M. Appl. Catal., A. 338 (2008) 52.

[14] Wu, P., Bai, P., Lei, Z., Loh, K. P., Zhao, X. S. Microporous and Mesoporous Materials. 141 (2011) 222.

[15] Zhu, K., Hu, J., Richards, R. Catal. Lett. 100 (2005) 195.

[16] Petcharoena, K., Sirivat, A. Mater. Sci. Eng. B. 177 (2012) 421.

[17] Anjana Pattnaik. Master of Science, National Institute of Technology, Rourkela (2011).

[18] Hakami, O., Zhang, Y., Banks, C. J. Water Res. 46 (2012) 3913.

[19] Khosroshahi, M. E., Ghazanfari, L. Mater. Chem. Phys. 133 (2012) 55.

[20] Zhan, G., Huang, J., Du, M., Sun, D., Ibrahim, A.-R., Lin, W., Hong, Y., Li, Q. Chem. Engin. J. 187 (2012) 232.

[21] Yang, X., Wang, X., Liang, C., Su, W., Wang, C., Feng, Z., Li, C., Qiu, J. Catal. Commun. 9 (2008) 2278.